

Quantification of cerebral perfusion using dynamic quantitative susceptibility mapping

Bo Xu^{1,2}, Pascal Spincemaille², Tian Xu³, Martin Prince², Silvina Dutruel², Ajay Gupta², Nandadeepa Thimmappa², and Yi Wang^{1,2}

¹Cornell University, New York, NY, United States, ²Weill Cornell Medical College, NY, United States, ³MedImageMetric LLC, NY, United States

Target Audience: Researchers interested in brain perfusion, contrast agent quantification and quantitative susceptibility mapping.

Purpose: Gd concentration ([Gd]) dynamic mapping is a required input to tracer kinetics model for generating tissue perfusion from contrast enhanced MRI (CEMRI). Traditional methods based on magnitude images suffer from saturation errors in high concentration and other biases [1,2], particularly in the estimation of the arterial input function (AIF). Recently developed quantitative susceptibility mapping (QSM) enables robust Gd estimation from phase images [2,3]. This study aims to develop a dynamic QSM technique with sufficient temporal resolution for mapping first pass [Gd] in CEMRI perfusion mapping.

Methods: 1) *Dynamic field map of the Gd passage:* A 3D 4-echo stack-spiral gradient echo sequence was developed with consecutive spirals interleaved by the golden ratio angle 220° . The spiral readout of one echo was refocused to the k-space center and flow compensated before the next echo [4]. Temporal Resolution Acceleration with Constrained Reconstruction (TRACER) [5] was used to reconstruct a temporal frame for each spiral increment after an initial full scan, resulting a 3D frame rate of $N_z \text{TR} \sim 748 \text{ms}$. The pre-Gd phase is subtracted from the later frames, and a dynamic mapping of the field of the Gd bolus passage was obtained by a linear fit of the phases across echoes.

2) *Perfusion mapping:* The Gd susceptibility map was converted to Gd concentration using the molar susceptibility of Gd^{3+} (308ppm L/mol) [7]. An AIF was chosen from the middle cerebral artery. A CBF map was computed using an SVD deconvolution [8] and a CBV map was computed by taking the ratio of concentration time integral of tissue and AIF [9].

3) *In vivo study:* This study was IRB approved and HIPAA-compliant. Three healthy volunteers (2 male, 1 female) were scanned a 3T scanner using an 8-channel head coil and the 3D 4-echo stack-spiral sequence ($\text{TR}/\text{TE}_{\text{first}}/\text{TE}_{\text{last}} = 34.3/0.7/25.3 \text{ ms}$, $\text{BW} = \pm 125 \text{ kHz}$, $\text{FA} = 15^\circ$, matrix size = $200 \times 200 \times 22$, $\text{FOV} = 22 \text{cm}$ covering the brain with the middle cerebral artery as AIF, $\sim 2.5 \text{ min}$ scan time). Twenty seconds after scan initiation, 0.1mmol/kg gadobutrol followed by 30ml saline was injected at 3ml/s. An arterial spin labeling (ASL) scan was performed before contrast injection. Images from the two scans were co-registered with FSL toolbox.

Results: Fig 1 shows the measured CBF and CBV maps of five slices in the center of the brain. Fig 2 shows the comparison of CBF maps obtained from ASL and dynamic QSM. Mean and standard deviation of CBF from 8 ROIs (Fig.2) from frontal lobe (ROI 1, 2), optical radiation (ROI 3, 4) and temporal lobe (ROI 5, 6, 7, 8) are plotted in Fig 3, demonstrating good agreement between dynamic QSM and ASL.

Discussion: First pass [Gd] time curves can be quantified using a multi-echo spiral acquisition, constrained image reconstruction, and QSM. The dynamic [Gd] maps can be used to extract AIF and tissue concentration curves for quantitative perfusion. Under-estimated CBF value was found in the boundary of frontal lobe and temporal lobe, likely due to spiral artifacts caused by the highly inhomogeneous field and errors from susceptibility mapping. The straight sinus and sagittal sinus also appeared different possibly due to the tagging difference between ASL and dynamic QSM.

Conclusion: Dynamic QSM is feasible for generating quantitative perfusion mapping from phase data of CEMRI.

References: [1] Schabe et al. MRM 2009; 62:1477-1486, [2] de Rochefort et al. Med Phys 2008; 35:5328, [3] de Rochefort MRM 2010; 63(1): 194-206. [4] Xu et al. MRM, online pub, DOI: 10.1002/mrm.24937. [5] Xu et al. MRM 2013;69(2):370-381. [6] Liu et al. MRM 2013;69(2):467-476. [7] Wang Y. Principles of Magnetic Resonance Imaging 2012. 276 p. [8] Ostergaard et al. MRM 1996;36(5):715-725. . [9] Rempp et al. Radiology 1994;193:637-641.

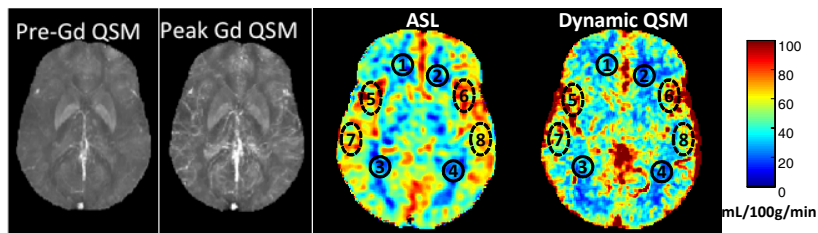


Fig 2. QSM pre-Gd and at peak Gd, and CBF from ASL and dynamic QSM

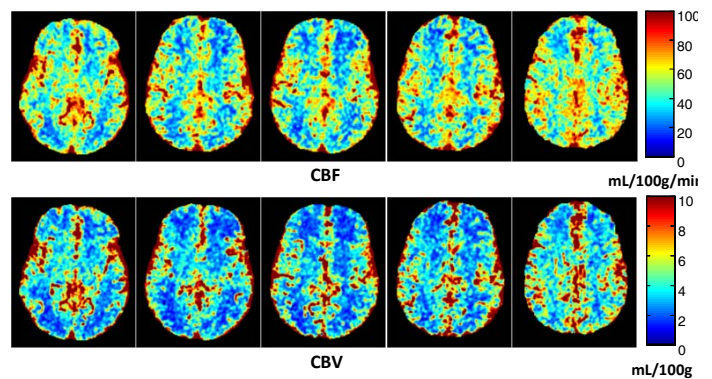


Fig 1. CBF and CBV maps computed from dQSM

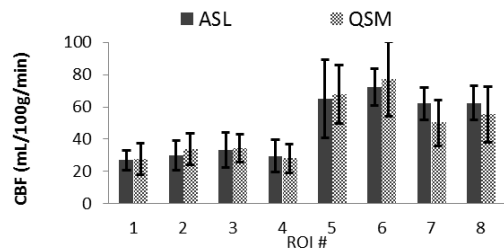


Fig 3. Comparison of CBF value between dQSM and ASL